Digest Journal of Nanomaterials and Biostructures Vol. 20, No. 4, October-December 2025, p. 1311-1324

Synthesis and physico-chemical characterization of WO_3-TiO_2 type composite materials for efficient electrochromic applications

R. Jothiramalingam [a,*], T. Radhika [b], V. N. Anjitha,[b], H. Al-Lohedan [a], A. Karami [a], S. Arokiyaraj [c]

[a] *Chemistry Department, College of Science, King Saud University, P.O. Box.2455, Riyadh 11451, Saudi Arabia.*

[b]*Center for Materials for Electronics Technology [C-MET], M.G. Kavu Thrissur, Kerala-680581, India.*

[c] *Department of Food Science and Biotechnology, Sejong University, South Korea*

In the present study ceramic mixed metal oxide such as WO_3 (tungsten trioxide) deposited Titania (TiO_2) in the form of composite was synthesized by sol-gel and hydrothermal method. The electrochromic application and physico chemical characteristic were demonstrated by powder X-ray diffraction (XRD), Raman and Ft-IR Spectroscopy method. The various weight percentage of tungsten trioxide deposited TiO_2 matrix have been studied for electrochromic applications. WO_3-Titania shows good activity and cycle performance up to 30 minutes was stable long standing at various potential applied on EC (Electrochromic device) device. The Scanning electron microscopy (SEM) and Transmission electron microscopy (TEM) reveals the morphology of square and circular particles formation for the prepared WO_3 and WO_3/TiO_2 nanoparticle. The EC device performance of the materials depends on the suitable composition of WT-1 with WO_3 on FTO plate and WT-2, WT-3 etc., depend on various factor the coloration as well as bleaching process obtained. The WO_3/TiO_2 (WT-1) in FTO plate on Electrochromic device shows long standing cycle stability and coloring and discoloration process.

(Received October 20, 2024; Accepted October 15, 2025)

Keywords: Tungsten trioxide, Nanoparticle,tiatani, Sol-gel process, Electrochromics

1. Introduction

Chromogenic materials are class of materials whose optical characteristic can be tuned reversibly under the impact of an external bias voltage. Such materials are capable of experiencing reversible color change and this phenomenon is known as chromism. In this process transition of electron in π- or d state occurs, which in turn causes alteration of color or constraints the transmission of light. The alteration in the optical characteristics reversible and is escorted by extraction and injection of ions and electrons under the impact of external electric field. This process is termed as electrochromism (EC). The alteration in color occurs either between two colored states or between a color state and bleached state. Recently, many devices are reported which works on the principle of electrochromism namely smart glasses, electrochromic mirrors and display devices. Electrochromic windows are capable of electrically tuning the emanation of the solar radiation, which is one of the sought-after technologies, which drastically lowers the energy requirements for air conditioning as well as for the purpose of indoor lighting. The parameters such as coloration efficiency, write-erase efficiency, high contrast ratio, low cost, flexible substrates, ecofriendly, multiple color states as well as precise response times, are required for EC device applications. Recently, plethora of materials has exhibited EC characteristics and among those transition metal oxides (TMOs) and conjugated polymers (CP) have obtained profound attention, but they are yet meet the later stated parameters. Among TMOs the TMOs based on W and Ni are widely investigated as they exhibit attractive EC characteristics. Further it is classified into two categories namely: cathodic and anodic. The cathodic materials undergo color change due to the insertion of

* Corresponding author: rjothiram@gmail.com
https://doi.org/10.15251/DJNB.2025.204.1311

ions, whereas an optical transition takes place in anodic materials owing to ion extraction. Few examples of cathodic materials which exhibits electrochromism are WO_3, TiO_2, Nb_2O_5 and MoO_3, while NiO, iridium oxide are few examples of Anodic EC materials. V_2O_5 is an example of intermediate EC oxide. Among all these WO_3 is widely covered and it portrays excellent EC properties. A typical Electrochromic device comprises of three constituents namely electrochromic material devices serve as active electrode (AE), a counter electrode (CE) and an electrolyte. In general, in visible range the CE is expected to exhibit higher transmittance, which facilitates the electrochemical reaction as it enhances the reaction kinetics. Further it is expected to have higher charge capacity which facilitates for insertion/ extraction of ions. This CE is found to be optically passive, as it transmittance is unaltered during the process of ion intercalation/de-intercalation, which in turn assists in circumventing interference with the coloration of electrochromic layer. This is sometimes called as ion storage layer (IS). Some devices comprise of cathodic EC layer and an anodic EC, such that color coating and bleach takes place concurrently. Electrolyte basically resides between electrochromic and ion storage layers (IS) which typically exhibit high ionic conductivity and lower electronic conductivity or ideally an insulator. It aims in providing mechanical support to the device. Additionally, it should not be reactive with electrodes between which it is placed, and should be chemically and thermal stable both during the time of preparation of the thin film and as well as device cycling. In smart windows application it is even desired to remain stable under solar radiation. It is observed that the EC displays are power efficient as well as cheap and it basically functions in two modes namely reflecting and transmitting.

The exiting characteristic which evaluates the capability of electrochromic materials is contrast ratio and this definition refers to the **contrast ratio** of a reflective display, specifically for displays that switch between a bleached (light or white) state and a colored (dark) state. The materials possessing higher contrast ratio is ideal for commercial uses. This parameter is crucial in evaluating the performance of displays like e-ink or electrochromic devices, where readability and visibility are dependent on their ability to achieve distinct contrast levels under ambient lighting. Keeping in view of the requirement of the higher contrast ratio of the electro chromatic device fabrication in this work, This method is used for synthesizing the WO_3-modified TiO_2 composite. The absence of surfactants simplifies the process and avoids contamination, ensuring high purity and better control over the material's morphology and properties. The electrochromic layer is placed in front of a diffusely scattering surface. This design enhances the display's visibility by scattering light, improving readability in various lighting conditions.

2. Materials and method

All chemicals such as $Na_2WO_4.2H_2O$, Titanium (IV) butoxide -TBO (Aldrich –Steinheim), Urea [$CO(NH_2)_2$] are used without further purification.

2.1. Preparation of WO_3

The precipitation method is adopted to make tungsten trioxide WO_3 using $Na_2WO_4.2H_2O$ (0.05M) and $H_2C_2O_4.2H_2O$ (0.125M) were dissolved in distilled water. As prepared 6M HCl was added to it and stirred for about 10 minutes until a clear solution is obtained. Hydrothermal process is carried out at proper condition (423 K for 72 h). The obtained material is wasted and dried in air for further study.

2.2. Preparation of WO_3/TiO_2 (WT)

Preparation of tungsten trioxide modified titania is prepared using the same precursors such as $Na_2WO_4.2H_2O$ and $H_2C_2O_4.2H_2O$ are dissolved in 25 ml water followed by stirring. Only alteration is to add the solution of Titanium (IV) butoxide (TBO) dissolved in 6M HCl and it further added with constant stirring. The as prepared solution was transferred into a Teflon lined autoclave and Hydrothermal process is carried out at 423 K for 72 h. The obtained material is wasted and dried in air for further study. The WO_3/TiO_2 materials having different ratios (W:Ti) such as WT-1 (1:1) and WT-3 (1:3) were prepared by taking different concentrations of TBO.

2.3. Electrochromic device fabrication

A paste was made consisting of as prepared material, dispersant (ethyl cellulose) and solvent (Terpineol) in order to study the electro-chromic property. The material, dispersing agent and solvent is maintained as follow 0.05: 0.0075: 0.03g. FTO plates are used to coat as prepared materials, after deposited the paste and dried in an oven at 333 K.

2.4. Preparation of EC device

Prior to the cell construction, FTO glass was cleaned properly using Ultrasonic bath followed by drying in an oven. The paste prepared with the material was coated on the conducting side of two FTO glasses and dried. In between these two FTO glasses a parafilm was placed. Parafilm was removed in the portion of paste coated. The electrolyte was applied in between these two FTO glasses where the paste coated. The FTO glasses joined together and made an EC device.

3. Results & discussion

The powder XRD is carried out to study the crystalline size and phase composition of the pure WO_3, TiO_2 and WT samples. The XRD patterns of WO_3, TiO_2 and WT materials are shown in Fig 1.

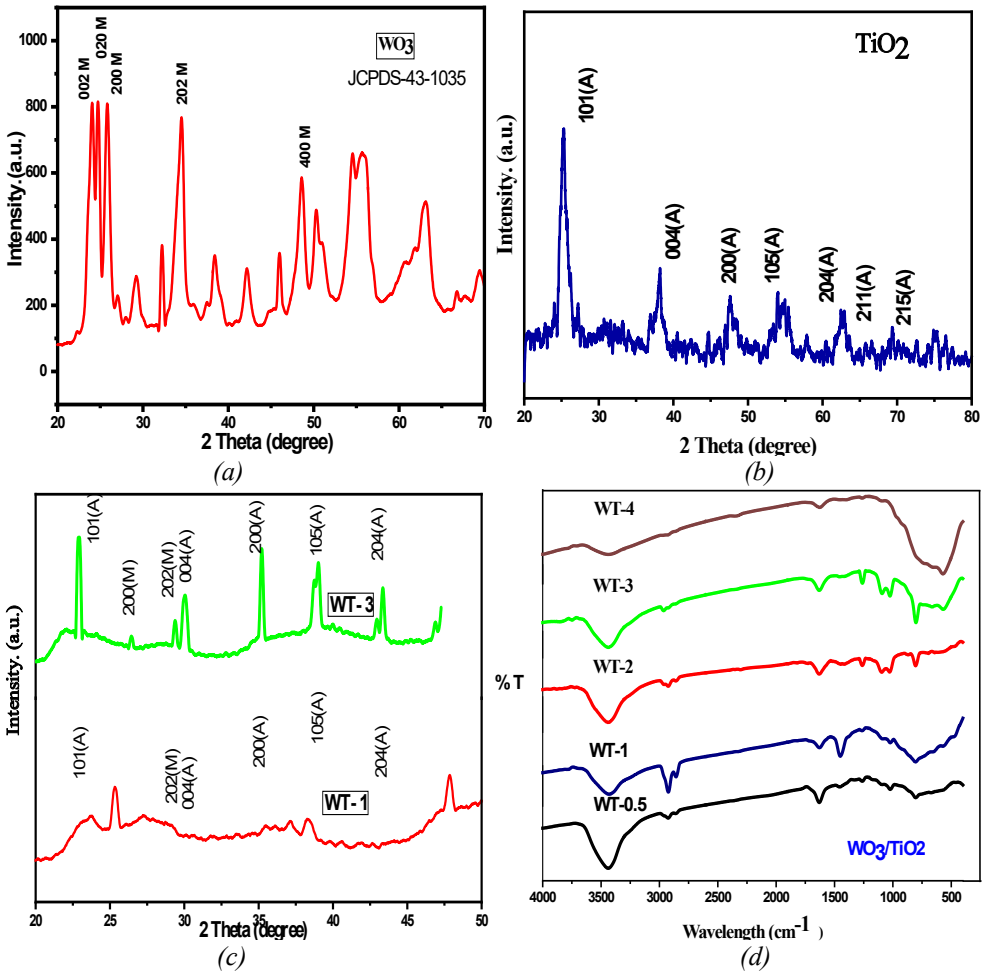

Fig. 1 (a-c) Powder XRD pattern of WO_3/TiO_2 and powder XRD pattern of WT materials with different W: Ti ratio.(d) FT-IR characterization of different ratio of WO_3/TiO_2.

The XRD pattern possesses well resolved futuristic characterization of monoclinic WO_3 with plane values of (002), (020), (200), and (202) are obtained. Thus, the WO_3 prepared shown purely monoclinic phase. In the case of monoclinic WO_3, lattice parameters are, a =7.297, b =7.539, and c =7.688 A° (JCPDS no. 43-1035). Powder XRD pattern obtained for TiO_2 prepared by hydrothermal method after calcination at 673 K is shown in Fig 1b. The XRD pattern possesses well resolved feature characteristics of anatase phase with planes and it showing following lattice parameters corresponding to anatase TiO_2, a = 3.78, b = 3.78 and c = 9.48. The pattern confirms the anatase phase in the hydrothermally prepared TiO_2 [3].

The diffraction peaks for anatase are associated with the (101) and (200) planes, with the (101) plane being the most intense, characteristic of the anatase crystal structure. MonoclinicWO_3, Peaks corresponding to (200) and (202) planes confirm the presence of monoclinic WO_3. The WT composites contain both monoclinic WO_3 and anatase TiO_2 phases, indicating successful integration of the two materials during synthesis. WT-3: Exhibits higher peak intensities for the anatase TiO_2 phase due to a greater concentration of TiO_2 in this sample. WT-1: Shows relatively lower anatase peak intensities, suggesting a lower proportion of TiO_2 in this sample. The coexistence of monoclinic WO_3 and anatase TiO_2 phases enhances the electrochromic and photocatalytic properties of the composite, as the two materials synergize to improve charge transfer and optical characteristics. The higher anatase content in WT-3 may result in improved optical transparency and photocatalytic activity, while WO_3 provides stability and better electrochromic performance. The XRD results confirm that the prepared WT materials successfully combine both monoclinic WO_3 and anatase TiO_2 phases, with varying proportions of TiO_2 affecting the overall material properties. The WT-3 sample, with a higher concentration of TiO_2, is likely more suitable for applications requiring a stronger anatase contribution, such as enhanced optical properties or photocatalysis.

3.2. Surface functional structure characterization

Stretching vibrations of W-O bonds: The bands between 1000-500 cm^{-1} are attributed to W-O stretching vibrations, specifically with a notable peak at 950 cm^{-1} for the W-O unit.

O-W-O vibrations: The peaks between 600-780 cm^{-1} are assigned to the vibrations of bridging oxygen atoms (O-W-O). This region indicates the structural organization of WO_3.

Hydroxyl and water-related peaks: The peaks at 1626 cm^{-1} and around 3400 cm^{-1} are linked to adsorbed water and hydroxyl groups, common in materials that have been synthesized hydrothermally or calcined, showing the presence of surface water or hydroxyl groups.

WO_6 vibrations: In the region of 1000-400 cm^{-1}, the vibrations of the WO_6 octahedra dominate, with distinct corner-sharing W-O-W stretching at 667 cm^{-1} and edge-sharing at 800 cm^{-1}. Broad absorption at ~3240 cm^{-1}: This is due to the stretching vibrations of surface-adsorbed water, which corresponds to bending vibrations observed around 1618 cm^{-1}. The overall FT-IR spectrum indicates the successful formation of monoclinic WO_3 under the hydrothermal synthesis and calcination at 673 K, confirming its structural features as represented by the characteristic vibrational bands.

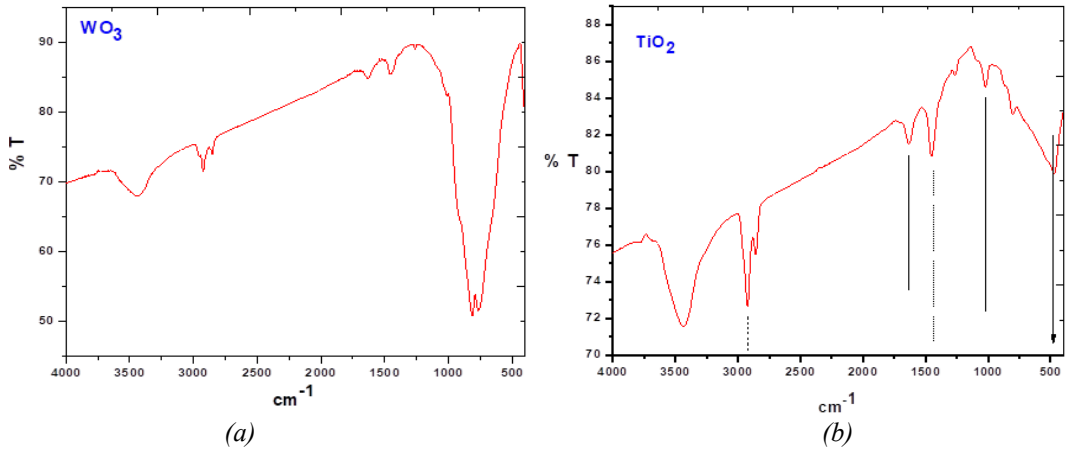

Fig. 2. Ft-IR Spectrum of as prepared WO_3 (a) and TiO_2 (b).

The Ft-IR spectrum of as prepared TiO_2 shows the stretching frequency in the range of 400-4000 cm^{-1} is given in Fig 2b. The Ft-IR spectra of TiO_2 and WO_3-TiO_2 (WT) materials provide important information about their structural characteristics and the presence of functional groups. TiO_2 Spectrum, Ti-O-Ti Stretching (~469 cm^{-1}): This band is associated with the Ti-O-Ti stretching vibration in TiO_2, confirming the presence of the anatase phase. Water Adsorption (~1640 cm^{-1}): The band at ~1640 cm^{-1} is attributed to the bending vibration of water molecules that are physically adsorbed on the surface of TiO_2, suggesting hydrophilicity. –OH Stretching (3500-2800 cm^{-1}): This region corresponds to the stretching vibrations of surface hydroxyl (-OH) groups, which are polar and give rise to strong IR absorption bands. CO_2 Adsorption (~2363 cm^{-1}): The presence of this band indicates that CO_2 from the atmosphere is adsorbed on the TiO_2 surface.

Absence of Alkoxide Peaks (1100-1000 cm^{-1}): The lack of a peak in this region confirms that the precursor alkoxide has been completely hydrolyzed to TiO_2 nanoparticles during the calcination process. The as prepard WT Materials Spectrum demonstrate Ti-O-Ti Stretching (~568 cm^{-1}): The band at 568 cm^{-1} appears in all WT materials, indicating the presence of Ti-O-Ti bonding, which is a signature of the TiO_2 phase. WO_3 Bands: W-O-W edge- and corner sharing (667 and 800 cm^{-1}). The band at 667 cm^{-1} and 800 cm^{-1} are attributed to the edge-sharing and corner-sharing W-O-W units in the WO_6 octahedra, characteristic of monoclinic WO_3. W=O Stretching (1019 cm^{-1}): This band corresponds to the W=O stretching vibration, suggesting the presence of W in an oxidized state.

W-O-W Bending (1094 cm^{-1}): This band is related to the bending vibrations of W-O-W in WO_6. O-W-O Stretching (1261 cm^{-1}): The band at 1261 cm^{-1} is attributed to O-W-O stretching vibrations, typical for WO_3. Water Bending (~1627 cm^{-1}): This band is linked to the bending vibrations of adsorbed water molecules. O-H Stretching (~2963 and 3441 cm^{-1}) peaks correspond to the stretching vibration of O-H groups from adsorbed water or surface hydroxyl group.

Hence, the Ft-IR spectra of the WT materials strongly suggest the presence of both monoclinic WO_3 and anatase TiO_2 phases. The absence of bands corresponding to W-O-Ti vibrations indicates no direct bonding between W and Ti in the materials, confirming that the formation of WT materials occurred under hydrothermal conditions without the formation of a Ti-W hybrid phase. Overall, the FT-IR analysis confirms that the WT materials are a mixture of monoclinic WO_3 and anatase TiO_2, with distinct surface characteristics related to adsorbed water and hydroxyl groups.

3.3. SEM-EDX characterizations

Figure 3 shows scanning electron microscope (SEM) images and its EDX spectrum of hydrothermally prepared WT-4 nanoparticles.

The SE micrographs of and its morphology of WT-4 nanoparticles show clear separation between their shapes of particle formation towards crystal structures of WO_3 and TiO_2. The material is largely consisting of square and small circular particles, in which the square like particles due to monoclinic (WO_3) and small spherical particles belong to anatase TiO_2 as depicted in Fig 3a. EDX analysis confirms the presence of elements W, Ti, and O as shown inset of the figure 3(c).

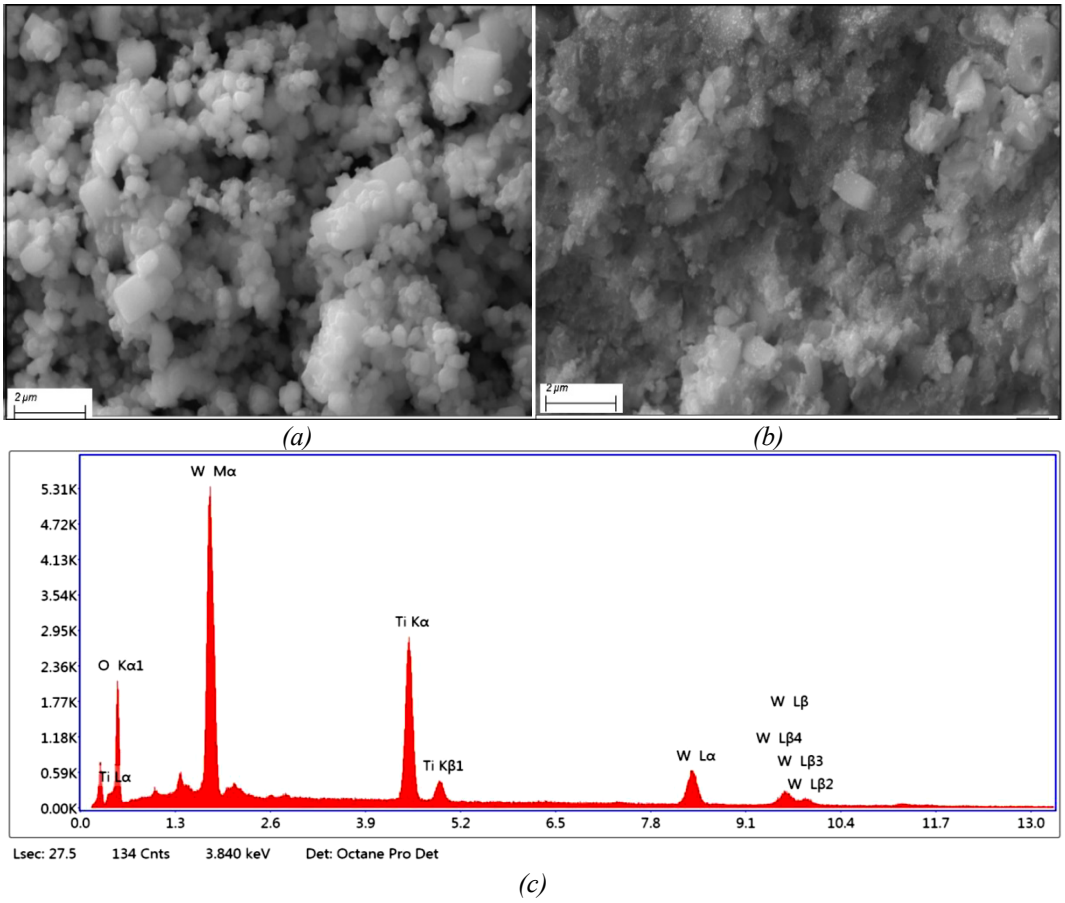

Fig. 3 (a and b) SEM-EDX images of WT- 4 material.

3.4. HR-TEM Analysis of pristine WO_3 and WO_3/TiO_2 nanoparticles

The TEM analysis of as prepared WO_3 and WT materials calcined at 673K is shown in Figure 4(a-c) and Figure 5. The TEM images of WO_3 forms the monoclinic WO_3, consist of number of squares shaped particles in the reported literature report. The TEM image as shown in Fig 4 representing the ladder shaped edges of monoclinic WO_3, and its high-resolution transmission electron microscope image images confirms the formation of square type particle with size range of 250-300 nm. The SAED pattern as shown in Fig 4d showing its polycrystalline nature and the EDAX confirms the presence of elements W and O. The TEM images of as prepared WT-3 calcined at 673K as shown below in Figure 5. The TEM images of WO_3 as shown in Fig 5a confirms the presence of uniform spherical anatase TiO_2 bonded on the surface of monoclinic WO_3, consist of number of squares above which the TiO_2 particle get attached. The TEM image as shown in Fig. 5a and 5c, Representing its high resolution - transmission electron microscope image of WT nanoparticles. The SAED pattern as shown in Fig 5b showing its polycrystalline nature and the Fig. 5d EDAX confirms the presence of elements W, Ti and O. Figure 5c and 5e shows the comparative TEM and SEM images of WT materials prepared in the present study. The square type particle formation occurred together with aggregated morphology. Cubic shapes of WO3 dispersed in the glassy film morphology of TiO_2 surface.

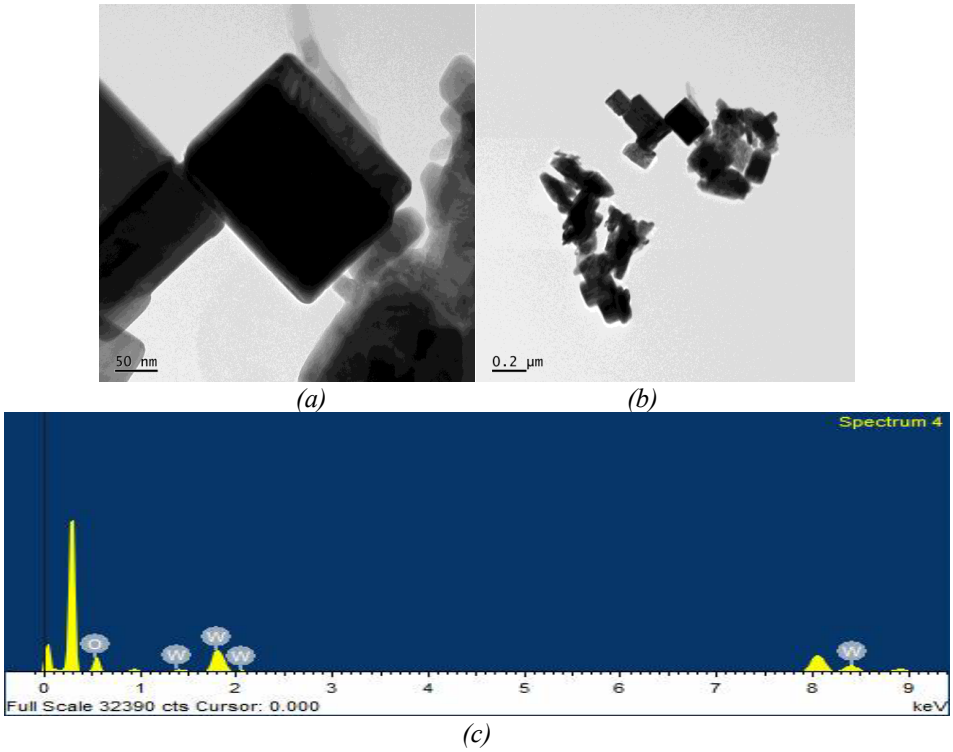

(a) *(b)*

(c)

Fig. 4 HR-TEM and EDX analysis of Tungsten oxide (WO3) prepared by hydrothermal process.

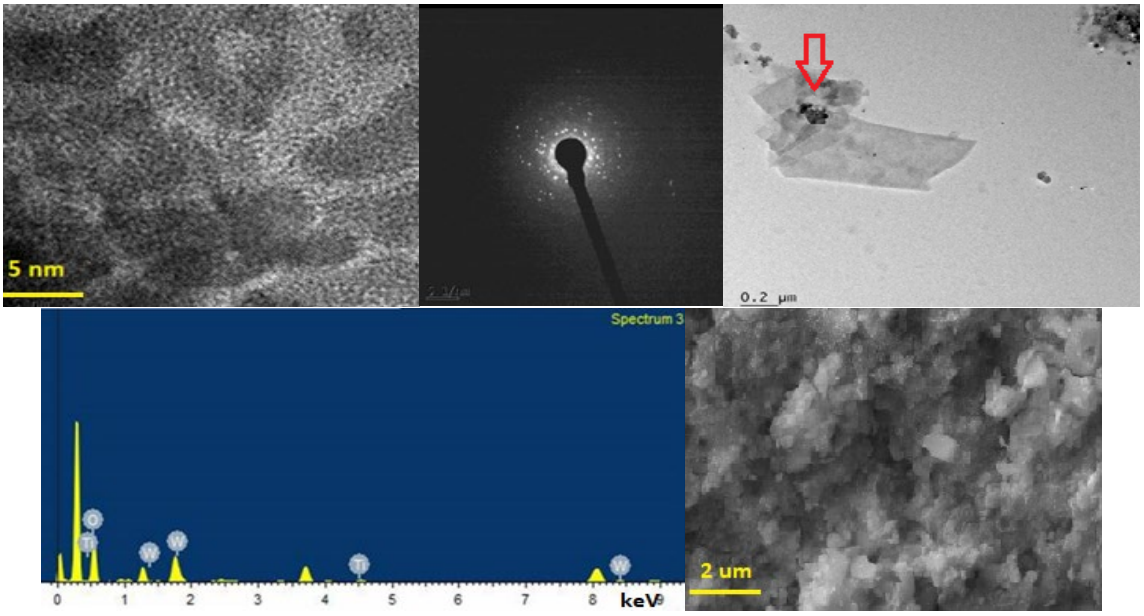

Fig. 5. (a-e) HR-TEM and EDX analysis of Tungsten oxide impregnated anatase form of titania (WT-3).

3.5. EC Property evaluation

The EC device was connected to a DC source and a multimeter. From DC source potential ranging from 0 V to 6 V was applied across it and the coloration process started. The Fig 25. shows the forward connection given to the EC device for coloration. For evaluating the bleaching process of EC device, the polarity given to the cell was reversed and the potential ranging from -6 V to -1 V was applied. Fig 6. shows reversing the polarity for bleaching process.

The variations in development of colors with different potentials for various EC devices constructed using different pastes are presented in the Tables 4.1- 4.

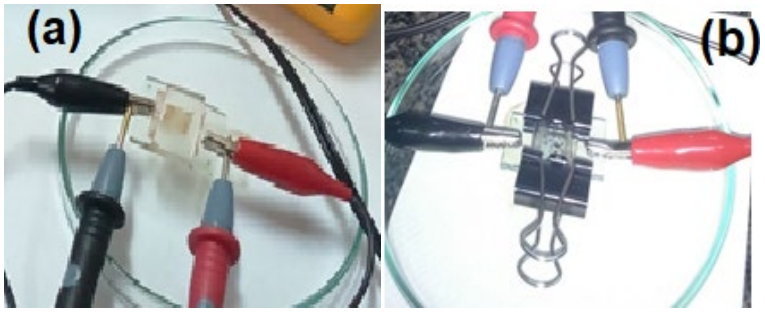

Fig. 6. (a) Forward connection for coloration (b) Reversing the polarity.

EC Device 1: Paste - WO_3 (FTO 1 and FTO 2)
Coloration

Time (min)	Potential (V)	Observed Color	EC Device
5	0	Light yellow	
10	2	Light blue	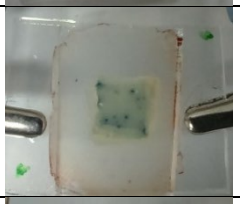
15	3	Blue	
20	4	Blue	
25	5	Deep blue	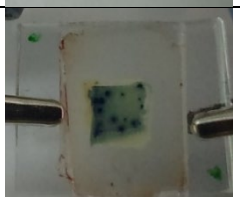
30	6	Deep blue	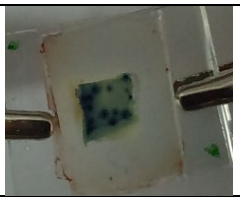

Bleaching

Time (min)	Potential(V)	Observed Color	EC Device
5	-6	Slight blue	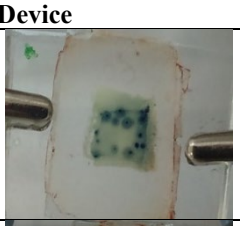
10	-3	Reduced blue	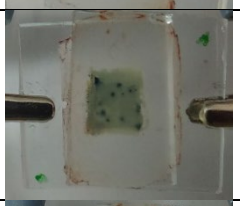
15	-1	Transparent	

The EC Device 1 made using calcined WO_3 paste shows good coloration with the applied voltage. The color changes from light yellow to light blue when 2 V is applied and shows deep blue color when 5 V is applied. When potential is reversed the color, intensity is also decreased and at -1 V the color became almost transparent. It is reversible. That is, it shows good electrochromic property.

The electrochromic properties of the material were analyzed using UV-Visible spectroscopy, focusing on the changes in transmittance during the coloration and bleaching processes, In the bleaching phase, the material reverts to its bleached (transparent) state by releasing ions from the electrochromic layer, returning to a more oxidized state. The decrease in transmittance during coloration and the increase during bleaching, as shown in the UV-Vis spectra, confirm the material's suitability for electrochromic applications. These properties underline its potential use in devices requiring efficient and reversible optical modulation with low power consumption.

Figure 7 shows the absorption and transmission UV-Vis spectra during coloration and bleaching transition.

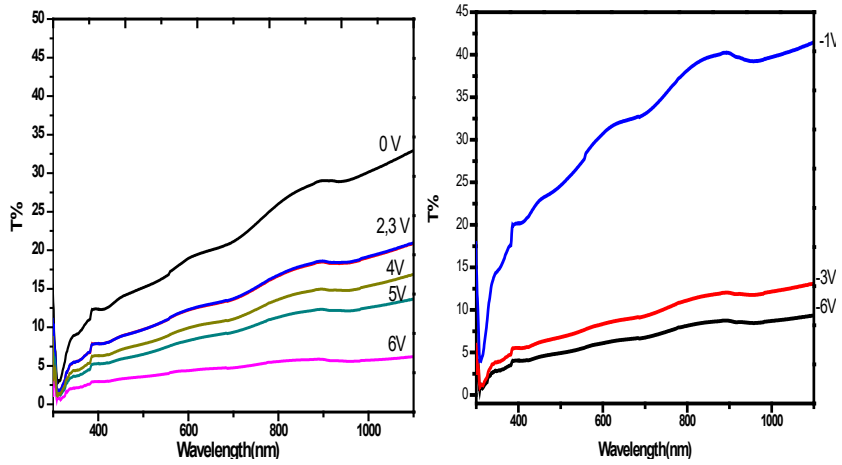

Fig. 7. Spectra for coloration and bleaching for EC device of WO_3.

1320

EC Device 2: Paste – WT- 2 (FTO 1 and FTO 2)

Coloration

Time (min)	Potential (V)	Observed Color	EC Device
5	0	Light yellow	
10	2	Light yellow	
15	3	Light Blue dots	
20	4	Blue dots	
25	5	Blue dots	
30	6	Blue dots	

Bleaching

Time (min)	Potential(V)	Observed Color	EC Device
5	-6	Reduced blue dots	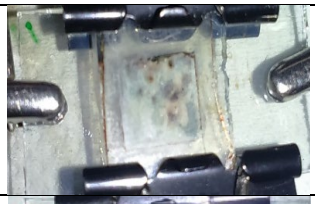
10	-3	Light Blue dots	

Time (min)	Potential(V)	Observed Color	EC Device
15	-1	One light blue dot	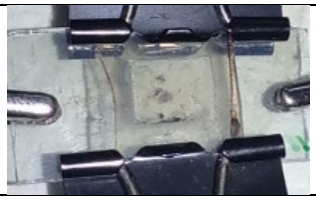

EC Device 2 shows less coloration. The color changes from light yellow to blue. The color developed in the form of dark dots and it didn't show any uniformity. It showing non uniform and less electrochromic property.

EC Device 3: Paste - dried WO_3 (FTO 1) and Paste - TiO_2 (FTO 2)
Coloration

Time (min)	Potential (V)	Observed Color	EC Device
5	0	V= 0; Red (color of electrolyte)	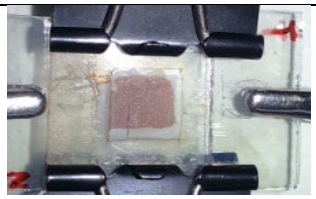
10	2	Red (color of electrolyte)	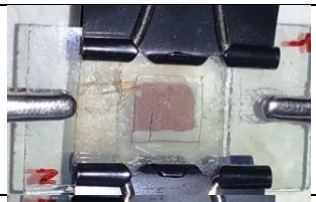
15	3	Light brown	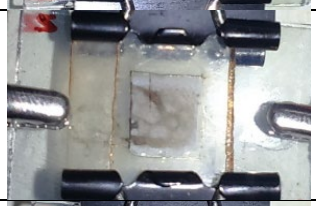
20	4	Light brown	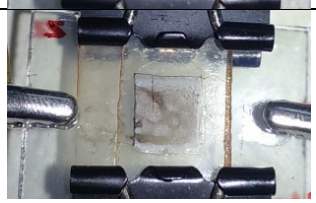
25	5	Brown line	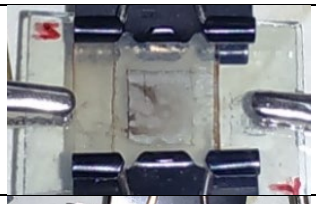
30	6	Dark brown line	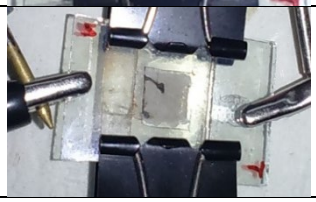

Bleaching

Time (min)	Potential(V)	Observed Color	EC Device
5	-6	Reduced brown line	
10	-3	Brown line	
15	-1	Brown line	

EC Device 3 shows little electrochromic property. The color change exhibited from red to brown and shows very less bleaching property.

The light blue color is appeared when 3 V is applied. That is, it requires more potential to initiate the coloration. It shows deep blue color when 6 V is applied. Hence from the overall analysis, The pure WO_3, WT-1 and WT-3 shows much better performance due to uniform charge charier transformation in the surface of TiO_2. Further studies are required to produce large scale synthesis of uniform coating on base metal oxide support. The mechanism behind the coloring and bleaching process in the TiO_2-WO_3 system can be explained by a combination of charge transfer, electron excitation, and intervalence electron transfer, which collectively enhance charge separation and color formation. Wide Bandgap of TiO_2: TiO_2 has a wide bandgap, making it difficult to excite electrons under normal conditions. However, WO_3 has a smaller bandgap, allowing electron excitation with an applied potential (electrochromic or photocatalytic process). Electron Excitation in WO_3: When a potential is applied or light is absorbed, electrons are excited from the valence band to the conduction band of WO_3. This process leaves behind holes in the valence band of WO_3. Hole Transfer from WO_3 to TiO_2: The hole created in the WO_3 valence band can be transferred to the conduction band of TiO_2. This process enhances charge separation, preventing electron-hole recombination and increasing color formation efficiency. Electron Transfer from WO_3 to TiO_2: Simultaneously, the electron excited in the conduction band of WO_3 can be transferred to the conduction band of TiO_2. This further improves charge separation, which is crucial for the coloring process. F-Center Activation by Defects and F-Centers: The defects in the TiO_2 lattice and WO_3 lattice (e.g., oxygen vacancies) can act as F-color centers (electron-trapping sites). These defects allow trapped electrons to absorb light, leading to a color change. The presence of multivalence tungsten species ($W^{6+}/W^{5+}/W^{4+}$) interacting with these defects further activates the color center formation, enhancing the overall chromic effect. Coloring and Bleaching:When an external potential is applied, or light is absorbed, electron transfer and charge separation lead to a buildup of charges that induce the coloration of the material due to electron trapping and intervalence charge transfer. Bleaching: When the applied potential is reversed, or in the absence of light, the electrons recombine with holes, and the material returns to its original state (bleaching), leading to the disappearance of color. These processes enhance the efficiency of color formation and bleaching by stabilizing charges and preventing recombination, thus making the system more effective for applications like smart windows, sensors, or displays.

5. Conclusions

The electrochromic property of the prepared materials was studied by examining the variations in development of colors with different potentials for various EC devices constructed using different pastes. The present work emphasizes on the preparation of materials such as WO_3, TiO_2, WO_3/TiO_2 composite. Hydrothermal and precipitation methods have adopted to prepared the all materials. The XRD, FT-IR and microscopy analysis confirms the physical bonding characteristics. The electron micrographic analysis further confirms the formation nanostructures of the as prepared material with square and spheres like aggregated particle morphology. The various composition addition of metal oxide in electrochromic device was studied and it shows the different coloring and bleaching properties with respect to applied potential possibility of F colour centre alteration in WO3 lattice. Future studies need to upgrade the electrochromic properties of as prepared materials for low-cost large-scale production of the as prepared materials for renewable and smart city applications.

Acknowledgements

The author (Jothiramalingam Rajabathar) acknowledges and extending their appreciation to Deanship of Scientific research, for financial support through Ongoing Research Funding program (ORF-2025-354), King Saud University, Riyadh, Saudi Arabia

References

[1] T. Radhika, K.R. Anju, M.S. Silpa, R.J. Ramalingam, H.A. Al-Lohedan, J. Electron. Mater. 46 (2017) 4567-4574; https://doi.org/10.1007/s11664-017-5442-8

[2] R. Jothiramalingam, K. Mathankumar, M. Sundararajan, M. Sukumard, J. A. Dhanraj, R. Divya, H. A. Al-Lohedan, M. Chandrasekarang, D. M. Al-Dhayan, Journal of Ovonic Research, Volume 18, Number 2, March - April 2022; https://doi.org/10.15251/JOR.2022.182.167

[3] N. Ozer, C.M. Lampert, Sol. Energy Mater. Sol. Cells. 54 (1998) 147-156; https://doi.org/10.1016/S0927-0248(98)00065-8

[4] S. Balaji, Y. Djaoued, A.-S. Albert, R. Brüning, N. Beaudoin, J. Robichaud, J. Mater. Chem. 21 (2011) 3940-3948; https://doi.org/10.1039/c0jm03773g

[5] R. Jothi Ramalignam, Govindasami Periyasamia, Mohamed Ouladsmane, Zeid A. ALOthman, Prabhakarn Arunachalam, Tariq Altalhi, T. Radhika, Abdullah G. Alanazi, Journal of Alloys and Compounds, 857 (2021) 160072; https://doi.org/10.1016/j.jallcom.2021.160072

[6] M.S. Koo, X. Chen, K. Cho, T. An, W. Choi, Environ. Sci. Technol. 53 (2019) 9926-9936; https://doi.org/10.1021/acs.est.9b02401

[7] W.C. Oh, J.D. Na, M.R.U.D. Biswas, Carbon Nanostructures. 27 (2019) 762-769; https://doi.org/10.1080/1536383X.2019.1635587

[8] Y.-C. Nah, A. Ghicov, D. Kim, S. Berger, P. Schmuki, J. Am. Chem. Soc. 130 (2008) 16154-16155; https://doi.org/10.1021/ja807106y

[9] S. Yao, F. Qu, G. Wang, X. Wu, J. Alloys Compd. 724 (2017) 695-702; https://doi.org/10.1016/j.jallcom.2017.07.123

[10] M. Govindasamy, B. Subramanian, S.-F. Wang, S. Chinnapaiyan, R.J. Ramalingam, H.A. Al-lohedan, Ultrason.Sonochem. 56 (2019) 134-142; https://doi.org/10.1016/j.ultsonch.2019.03.021

[11] A. Verma, S.B. Samanta, A.K. Bakhshi, S.A. Agnihotry, Indian J. Chem. - Sect. A Inorganic, Phys. Theor. Anal. Chem. 44 (2005) 1756-1765.

[12] M.-J. Chen, H. Shen, Journal SouthChina Univ. Technol. (Natural Sci. 32 (2004) 31-35.

[13] M.B. Tahir, S. Ali, M. Rizwan, Int. J.Environ. Sci. Technol. 16 (2019) 4975-4988; https://doi.org/10.1007/s13762-019-02385-5

[14] S. Bogati, R. Basnet, W. Graf, A. Georg, Sol. EnergyMater. Sol. Cells. 166 (2017) 204-211; https://doi.org/10.1016/j.solmat.2017.03.020

[15] Y. Xiong, C. Wang, C. Jin, Q. Sun, M. Xu, ACS Sustain.Chem. Eng. 6 (2018) 13897-13906; https://doi.org/10.1021/acssuschemeng.8b02138

[16] H. Zhang, S. Wang, Y. Wang, J. Yang, X. Gao, L. Wang, Phys. Chem.Chem. Phys. 16 (2014) 10830-10836; https://doi.org/10.1039/C4CP00356J

[17] T.D. Nguyen, L.P. Yeo, D. Mandler, S. Magdassi, A.I. Yoong Tok, RSC Adv. 9 (2019) 16730-16737; https://doi.org/10.1039/C9RA03084K

[18] F. Zheng, C. Xi, J. Xu, Y. Yu, W. Yang, P. Hu, Y. Li, Q. Zhen, S. Bashir, J.L. Liu, J. Alloys Compd. 772 (2019) 933-942; https://doi.org/10.1016/j.jallcom.2018.09.085

[19] S. Bogati, A. Georg, W. Graf, Sol. Energy Mater. Sol. Cells. 163 (2017) 170-177; https://doi.org/10.1016/j.solmat.2017.01.016

[20] T. Radhika, Rajabathar Jothi Ramalingam, V. Aneesha,Munirah D. Albaqami, Optik - International Journal for Light and Electron Optics 228 (2021) 166145; https://doi.org/10.1016/j.ijleo.2020.166145